Biomechanics of the Distal Radioulnar Joint During In Vivo Forearm Pronosupination

Bardiya Akhbari, MSc[1] Kalpit N. Shah, MD[2] Amy M. Morton, MSc[2] Douglas C. Moore, MSc[2] Arnold-Peter C. Weiss, MD[2,3] Scott W. Wolfe, MD[4,5] Joseph J. Crisco, PhD[1,2]

[1] Center for Biomedical Engineering, Brown University, Providence, Rhode Island
[2] Department of Orthopedics, The Warren Alpert Medical School of Brown University and Rhode Island Hospital, Providence, Rhode Island
[3] Division of Hand, Upper Extremity & Microvascular Surgery, Department of Orthopaedics, The Warren Alpert Medical School of Brown University and Rhode Island Hospital, Providence, Rhode Island
[4] Hand and Upper Extremity Center, Hospital for Special Surgery, New York, New York
[5] Department of Orthopaedic Surgery, Weill Medical College of Cornell University, New York, New York

Address for correspondence Joseph J. Crisco, PhD, Bioengineering Laboratory, Department of Orthopedics, The Warren Alpert Medical School of Brown University and Rhode Island Hospital, 1 Hoppin Street, CORO West, Suite 404, Providence, RI 02903 (e-mail: joseph_crisco@brown.edu).

J Wrist Surg 2021;10:208–215.

Abstract

Background Ulnar variance (UV) and center of rotation (COR) location at the level of the distal radioulnar joint (DRUJ) change with forearm rotation. Nevertheless, these parameters have not been assessed dynamically during active in vivo pronosupination. This assessment could help us to improve our diagnosis and treatment strategies.

Questions/purposes We sought to (1) mathematically model the UV change, and (2) determine the dynamic COR's location during active pronosupination.

Methods We used biplanar videoradiography to study DRUJ during in vivo pronation and supination in nine healthy subjects. UV was defined as the proximal-distal distance of ulnar fovea with respect to the radial sigmoid notch, and COR was calculated using helical axis of motion parameters. The continuous change of UV was evaluated using a generalized linear regression model.

Results A second-degree polynomial with R^2 of 0.85 was able to model the UV changes. Maximum negative UV occurred at 38.0 degrees supination and maximum positive UV occurred at maximum pronation. At maximum pronation, the COR was located 0.5 ± 1.8 mm ulnarly and 0.6 ± 0.8 mm volarly from the center of the ulnar fovea, while at maximum supination, the COR was located 0.2 ± 0.6 mm radially and 2.0 ± 0.5 mm volarly.

Conclusion Changes in UV and volar translation of the COR are nonlinear at the DRUJ during pronosupination.

Clinical Relevance Understanding the dynamic nature of UV as a function of pronosupination can help guide accurate evaluation and treatment of wrist pathology where the UV is an important consideration. The dynamic behavior of COR might be useful in designing DRUJ replacement implants to match the anatomical motion.

Keywords
- radioulnar joint
- kinematics
- ulnar variance
- DRUJ
- center of rotation

received
August 28, 2020
accepted
November 12, 2020
published online
February 4, 2021

DOI https://doi.org/10.1055/s-0040-1722334.
ISSN 2163-3916.

The distal radioulnar joint (DRUJ) plays a critical role for both load-bearing and motion of the upper extremity.[1,2] Ulnar variance (UV), the relative distal-proximal position of the distal ulna with respect to the radius, is often assessed to evaluate the etiology of wrist pain. Positive UV has been associated with ulnocarpal impaction syndrome and central tears of the triangular fibrocartilage complex (TFCC), while negative UV has been linked to Kienböck disease.[3–6] Additionally, the load seen across the ulnocarpal joint varies with even slight changes in UV. In a cadaveric study, Palmer and Werner demonstrated that a 2.5 mm change in UV decreases the load at the ulnocarpal joint from 18 to 4% when the ulna is shortened, but increases from 18 to 42% when the ulna is lengthened.[7]

Pathology involving the DRUJ often leads to pain and instability, which in severe cases- may require surgical interventions, such as ligament repair or reconstruction, resection, fusion, and, more recently, joint replacement.[8–13] Successful joint arthroplasty designs in shoulder, hip, and knee have shown the importance of implant design to reproduce healthy joint kinematics.[14–17] Biomechanical studies of the healthy DRUJ have reported that the location of the center of rotation (COR) is not fixed during forearm pronosupination[18,19] and that it moves volarly and ulnarly with elbow extension.[20] However, linked DRUJ implants that replace the sigmoid notch and ulnar head often employ a ball-and-socket design[8,11,12] which has a fixed COR at the center of the replacement ulnar head. Current DRUJ replacement provides pain relief and has an encouraging success rate, but it also suffers from a high complication rate (35% in 8 years) including periprosthetic fractures or continued instability after the surgery.[8,21] Although the reasons for complications are highly debated, abnormal kinematics may lead to increased implant-bone stress. Therefore, accurate in vivo evaluation of COR movement could help us to better understand normal kinematics and may help advance implant designs.

Although previous studies have demonstrated the change in UV[22–24] and COR[19,25] at different forearm rotation angles, they have not assessed their continuous changes throughout in vivo forearm pronation-supination (PS). Biplanar videoradiography (BVR) is an imaging technique that is used for computing the in vivo motion of other joints with high accuracy.[26–33] Thus, in this study, we used a BVR system to evaluate the mechanism of motion of DRUJ by analyzing specifically (1) UV and (2) COR during active pronosupination. We hypothesized that UV would be most positive at full pronation and that it would reduce as the forearm rotates towards full supination, where it would reach its minimum value. We also hypothesized that the COR is not stationary throughout pronosupination.

Methods

Subjects and In Vivo Imaging

Nine subjects (eight females, eight right-hand dominant, 56.9 ± 5.5 years) with no history of wrist or hand pathology were enrolled after Institutional Review Board approval as part of a larger study on wrist and forearm kinematics.[34] Computed tomography (CT) scans (Lightspeed 16, GE Medical, Milwaukee, WI) were acquired of the distal forearm, wrist, and hand with tube settings of 80 kVp and 80 mA, and three-dimensional (3D) image resolution of $0.39 \times 0.39 \times 0.625\,mm^3$. The radius and ulna were semiautomatically segmented using commercially available medical image processing software (Mimics v19, Materialise NV, Leuven, BE), using a gradient-based algorithm.[35] The segmented portions of the images reflecting the bones were exported as CT image volumes containing the attenuation values for further processing in BVR, and they were also exported as 3D surface models for kinematics analysis.

Experimental Setup

BVR acquisition was performed at the X-ray Reconstruction of Moving Morphology (XROMM) facility at Brown University (►**Fig. 1**). The XROMM system consists of two Varian Medical Systems Model G-1086 X-ray tubes (Palo Alto, CA), two EMD Technologies model EPS 45 to 80 pulsed X-ray generators (Saint-Eustache, Quebec, QC), two 40-cm Dunlee (Aurora, IL) image intensifiers, and two Phantom v10 high-speed video cameras (Vision Research, Wayne, NJ). In this experiment, the angle between sources was 110 degrees, and the source-to-image distance was set at 130 cm. X-ray tube settings were adjusted between 68 and 75 kV and 80 mA, along with a continuous capture rate of 200 Hz and a shutter speed of 500 µs. The X-ray systems were calibrated, and radiographs were undistorted in XMALab software (Brown University, Providence, RI), using a previously described methodology.[36,37]

Prior to the in vivo experiment, the rotational and translational accuracies of model-based BVR tracking for the DRUJ were assessed using an experimental setup that has been described previously.[28] Briefly, accuracy was determined in a study involving five forearms from four cadavers (two females, three right and one both sides, 70.5 ± 13.2 years).

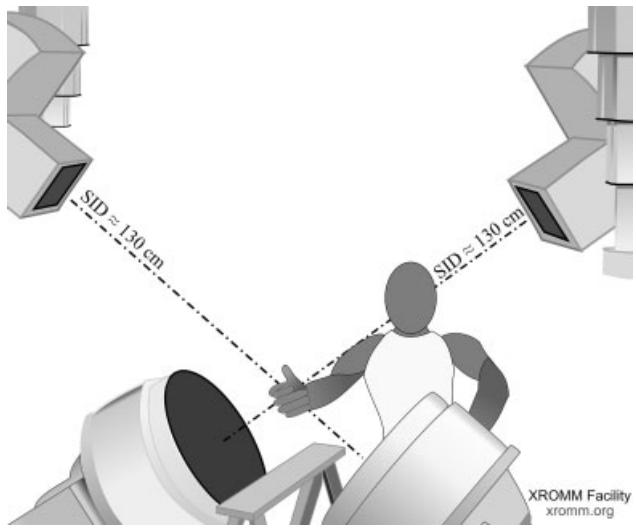

Fig. 1 The biplane videoradiography experimental setup. The orientation between sources was 110 degrees, and the source-to-hand distance was approximately 90 cm. A doorknob device was affixed to the trestle and subjects' wrist joint was at the center of the field-of-view of the X-ray sources.

DRUJ motion was simultaneously calculated using eight motion capture cameras (gold-standard) and the BVR system during pronation and supination tasks. DRUJ kinematics and UV were computed as described in the next section. Overall, the accuracy of calculating the position and orientation of DRUJ was less than 1 degree and 1 mm, and the accuracy of computing the UV throughout pronosupination of the forearm was between −0.5 and 0.7 mm.

Each study participant performed active forearm pronation and supination using a custom-designed T-handle doorknob fixture. The doorknob fixture was fabricated from a plastic shovel handle with two sizes to accommodate different sizes of hands. Subjects started the tasks from a functional neutral position (i.e., holding pose) and performed two repetitions of pronation and supination, after they were coached and practiced reaching their maximum pronation or supination rotation rates as quickly as possible. To minimize the radiation exposure to the subjects, each direction of motion was limited to 2 seconds (i.e., 400 radiographic images) recording. The mean total effective radiation dosage of these two tasks and the CT acquisition was 47 mrem, equivalent to 28 days of background radiation in the United States.[38]

Data Processing

Radial and ulnar coordinate systems (CS) were defined from the surface bone models using their anatomical landmarks, as previously described (►**Fig. 2**).[35,39,40] Briefly, the ulnar CS was defined with its x-axis along the ulnar shaft (positive proximally), and y-axis directed toward the ulnar notch but projected on the distal surface (positive radially). The origin was defined as the intersection of x-axis and the distal surface of the ulna (approximately at ulnar fovea). The radial CS's x-axis was defined in the direction of the radial shaft, and y-axis was toward the radial styloid projected to the articular surface of the radius with scaphoid.

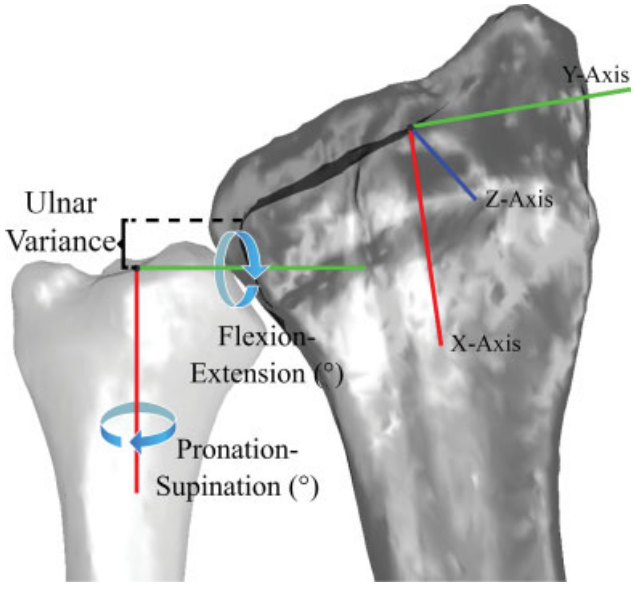

Fig. 2 The coordinate systems of the radius and ulna in volar view of the ulna. x-axis (directed proximally), y-axis (directed radially), and z-axis (directed volarly) are shown for both bones. The ulnar variance was defined as the proximal-distal distance between the ulna fovea (origin of the ulnar coordinate system) to the sigmoid notch of the radius at the neutral pose. In this figure, the ulnar variance is negative.

DRUJ motion was calculated by tracking the radius and ulna in the videoradiographs using open-source markerless 2D to 3D image registration software, as described previously (Autoscoper, Brown University, https://simtk.org/projects/autoscoper).[27,28] Briefly, digitally reconstructed radiographs (DRRs) were generated from the segmented CT volume images using a ray-casting approach, and both radius and ulna were tracked in the calibrated BVR space (►**Fig. 3**). Tracking was accomplished by minimizing a normalized cross-correlation cost function between the DRRs and the radiographs using the particle swarm optimization algorithm.[41] The kinematic transformation matrices of the tracked bones were then transformed to their anatomical CS, and the relative position of radius in ulnar CS was calculated.

Helical axis of motion (HAM) parameters[42] were calculated to describe the kinematics as the relative motion of radius CS in ulnar CS, with respect to the neutral pose. The HAM rotation was decomposed in the ulnar CS using the HAM screw axis, and the pronation (positive) and supination (negative) of forearm were calculated. The neutral pose was defined when PS was zero. UV was defined as the relative position of the ulnar fovea (as a constant point fixed to the ulnar head) with respect to the distal margin of the sigmoid notch on the radius (►**Fig. 2**). The COR location was defined as the intersection of the unique screw axis defined by HAM with the ulnar distal surface (yz-plane). The UV at the neutral pose for each subject was set to zero (0) to standardize changes as a function of PS.

Statistical Analysis

The full motion arc of the DRUJ and the dynamic behavior of UV were evaluated for all subjects. A generalized linear model was used to describe the relationship between the change in UV and PS ($UV = p_1 \times PS^2 + p_2 \times PS$), where p_1 and p_2 were coefficients that were optimized using linear regression. Adjusted R^2, and root-mean-square-error (RMSE) were calculated to define the robustness of the model, and 95% confidence intervals (CIs) were computed to describe the UV changes. The same model was also applied to the data for each individual to assure the robustness of the model in each subject. COR locations at each degree of PS were averaged across all subjects to demonstrate the dynamic change in the COR location as the forearm pronates and supinates.

Results

Average forearm pronation for the subjects we studied was 59.7 ± 11.8 degrees (range: 42.5–76.7 degrees) and average supination was 72.2 ± 11.1 degrees (55.3–92.1 degrees), for a total forearm pronosupination ROM of 131.9 ± 4.7 degrees (124.5–140.6 degrees). At the neutral position, UV was −1.6 ± 1.6 mm, while it was +1.3 ± 1.7 mm in maximum pronation and −1.8 ± 1.6 mm in maximum supination (►**Table 1**).

UV changed nonlinearly with pronosupination of the forearm (►**Fig. 4**). The change in UV was the most positive at full pronation (2.9–5.2 mm 95% CI, $p < 0.001$), but decreased during supination, with the lowest UV (−1.8 to 0.5 mm) noted at

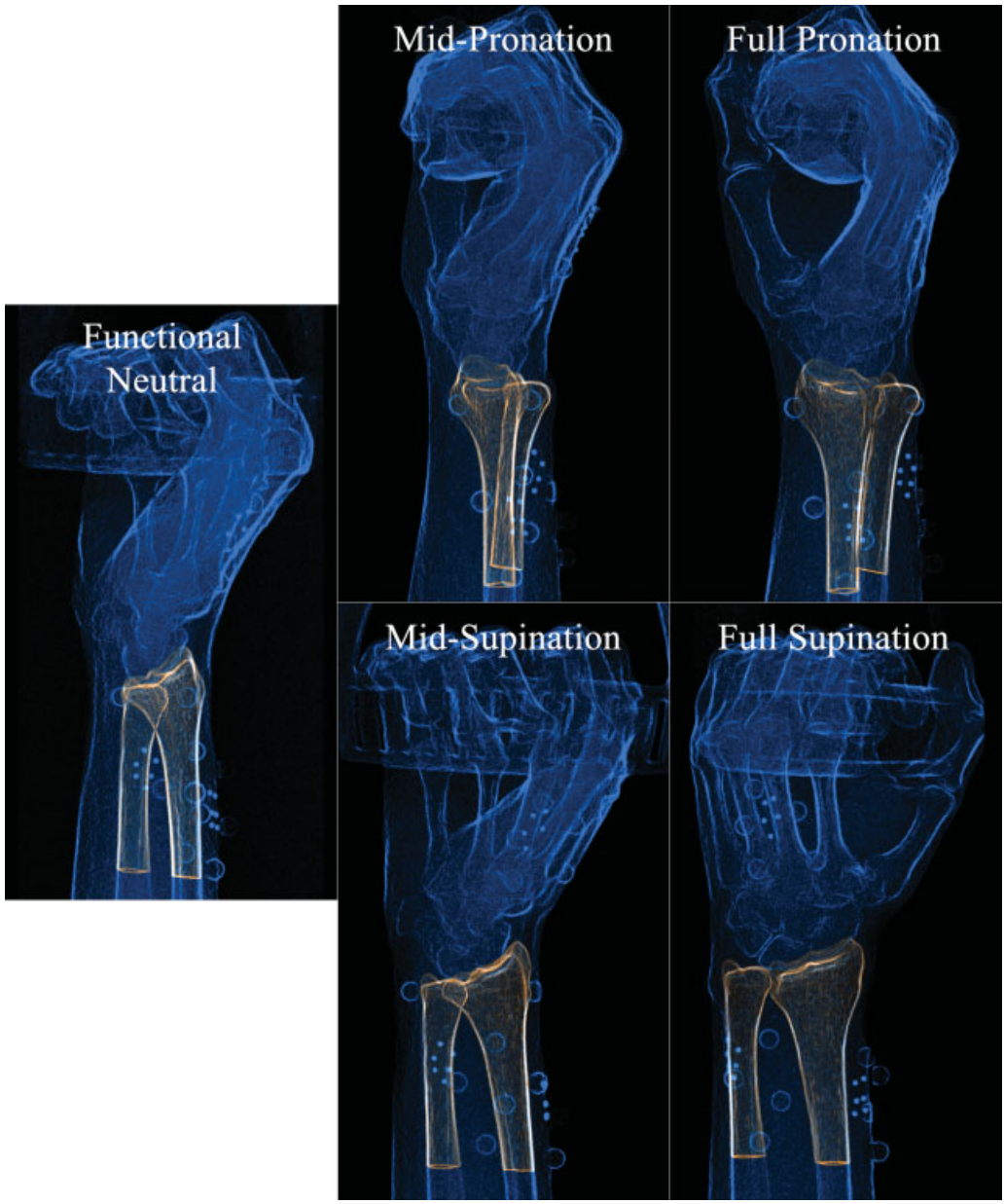

Fig. 3 Examples of tracked radius and ulna for one subject overlaid on one of the radiographs in the functional neutral position, mid- and full pronation (25 and 50 degrees), and mid- and full supination (30 and 60 degrees). The highlighted sections are the digitally reconstructed radiographs of the bones after tracking and optimization process. The features of the bones in the radiographs are enhanced using the Sobel and intensity image filters.

mid-supination (approximately 38.0 degrees). Interestingly, the lowest UV was observed at mid-supination, and it increased slightly from mid-supination to full supination for all subjects. This behavior was modeled as a second-degree polynomial with an average (95% CI) p_1 of 0.00033 (0.00032, 0.00034), and p_2 of 0.0276 (0.0273, 0.0278). The fitted equation had an adjusted R^2 of 0.85, and RMSE of 0.60 mm. The second order polynomial models fit the individual subjects UV values well with an adjusted R^2 that ranged from 0.85 to 0.99 and RMSEs that were less than 0.59 mm.

The COR was located 0.5 ± 1.8 mm ulnarly and 0.6 ± 0.8 mm volarly from the ulnar fovea in maximum pronation ($p > 0.05$), while in maximum supination the COR was located 0.2 ± 0.6 mm radially and 2.0 ± 0.5 mm volarly from the fovea (►**Figs. 5** and **6**). The dynamic nature of the shift in COR was observed from the neutral pose to maximum pronation, when the COR significantly moved volarly ($p < 0.0001$). There was no significant radial-ulnar translation for the COR ($p > 0.05$).

Discussion

Understanding how UV and COR change as the forearm pronates and supinates could help improve diagnosis and treatment strategies. In this study we used an accurate in vivo BVR technique and demonstrated the continuous change of UV during pronosupination from its most positive value at full pronation to its minimum occurring at approximately

Table 1 Maximum pronation and supination of the distal radioulnar joint during active motion, and associated ulnar variance at the neutral position and maximum pronation-supination for all subjects. Note that the most negative UV did not occur at maximum supination (see ►**Fig. 4**)

Subjects	Ulnar variance at neutral (mm)	Maximum pronation (degrees)	Ulnar variance at maximum pronation (mm)	Maximum supination (degrees)	Ulnar variance at maximum supination (mm)
S1	−1.8	61.0	1.4	67.6	−3.0
S2	−0.8	43.1	1.7	92.9	−1.3
S3	−2.5	57.6	0.1	75.8	−2.1
S4	−2.1	73.3	1.7	54.8	−2.8
S5	−4.1	76.6	−1.5	64.3	−3.6
S6	−1.9	58.8	1.2	75.6	−2.4
S7	−1.7	48.9	1.1	82.0	−1.4
S8	−1.2	71.5	0.8	63.3	−1.8
S9	2.0	52.0	5.1	72.8	1.9
Mean (SD)	*−1.6 (1.6)*	*60.3 (11.5)*	*1.3 (1.7)*	*72.1 (11.3)*	*−1.8 (1.6)*

Note: Ulnar variance was negative for all subjects except one, and ulnar variance at the maximum supination was approximately equal to its value at the neutral pose.

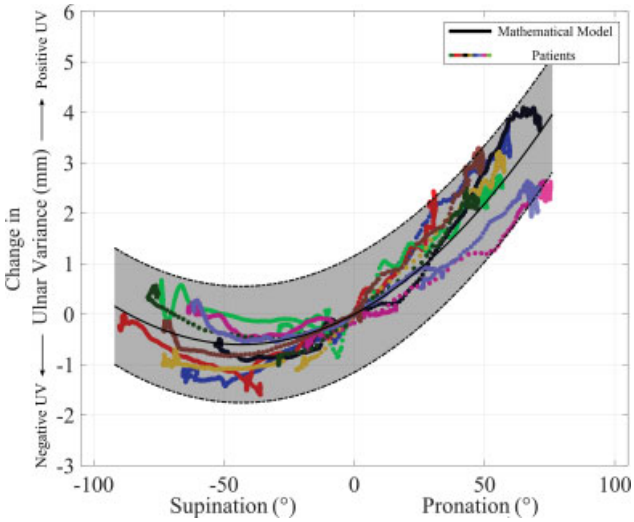

Fig. 4 The change in ulnar variance (UV) from its value at the neutral position was nonlinear relative to forearm pronosupination. The most negative UV was noted at an average of 38.0 degrees of supination. The solid line is demonstrating the fitted model, and shaded area are demonstrating its 95% confidence interval.

38 degrees of supination, instead of full supination. Previous reports have demonstrated that UV decreases as the forearm goes from pronation to supination,[22,43] but this study is the first in vivo study to demonstrate the nonlinear relationship of these changes. We also demonstrated that the nature of COR is dynamic in supination.

Clinically, the finding that UV is the most negative at about half supination has implications in immobilization following stabilization procedures for the DRUJ or treatments of TFCC tears by arthroscopic or open means. Traditionally, immobilization has been in long arm splints with the forearm fully supinated; it stands to reason, based on our findings, that optimal immobilization of rotation following reconstructive procedures may be best at 40 to 45 degrees of supination to reduce DRUJ/TFCC stress.

By investigating the continuous pattern of change in UV, we provided an equation that could be useful in standardizing UV measures. Although a standard methodology for measuring UV exists,[44] the literature varies with regard to wrist and forearm position when radiographically assessing the UV,[22] which can directly impact the measurement.[20,23,24] We calculated the UV at the neutral forearm rotation pose and then evaluated the changes seen in the UV during PS compared with the neutral. The nonlinear behavior of UV could be informed by the previously described piston-like motion of the radius on the ulna.[1] We believe that the tilt on radial head and the inherent geometrical constraint of the proximal radioulnar joint are causing the radius to cross the ulna in a triangle-like form, resulting in this nonlinear pattern and producing positive UV. This nonlinear pattern might also correspond to how ulna "seats" into the sigmoid notch in full supination, and the fact that extensor carpi ulnaris is straight and dorsal above the ulna in this position.

Earlier studies have evaluated UV at only discreet postures, and they have been prone to errors due to the subjective measurement variations among the operators. However, in this study UV was measured continuously and accurately using objective metrics from 3D models for each subject. Previously, Epner et al studied seven cadaveric wrists and demonstrated that the UV becomes 1 mm more negative when the forearm rotates from pronation to supination.[22] However, the range of this change was between 0 and 2.1 mm leading to an inability to make conclusive statements. Jung et al studied 120 radiographs of healthy wrists in a power grip posture and found an overall weak linear relationship ($R^2 = 0.07$) between UV and forearm pronosupination, decreasing from $+1.5 \pm 1.6$ mm in full pronation to $+0.9 \pm 1.5$ mm in full supination. However, the authors only measured UV at maximum pronation and

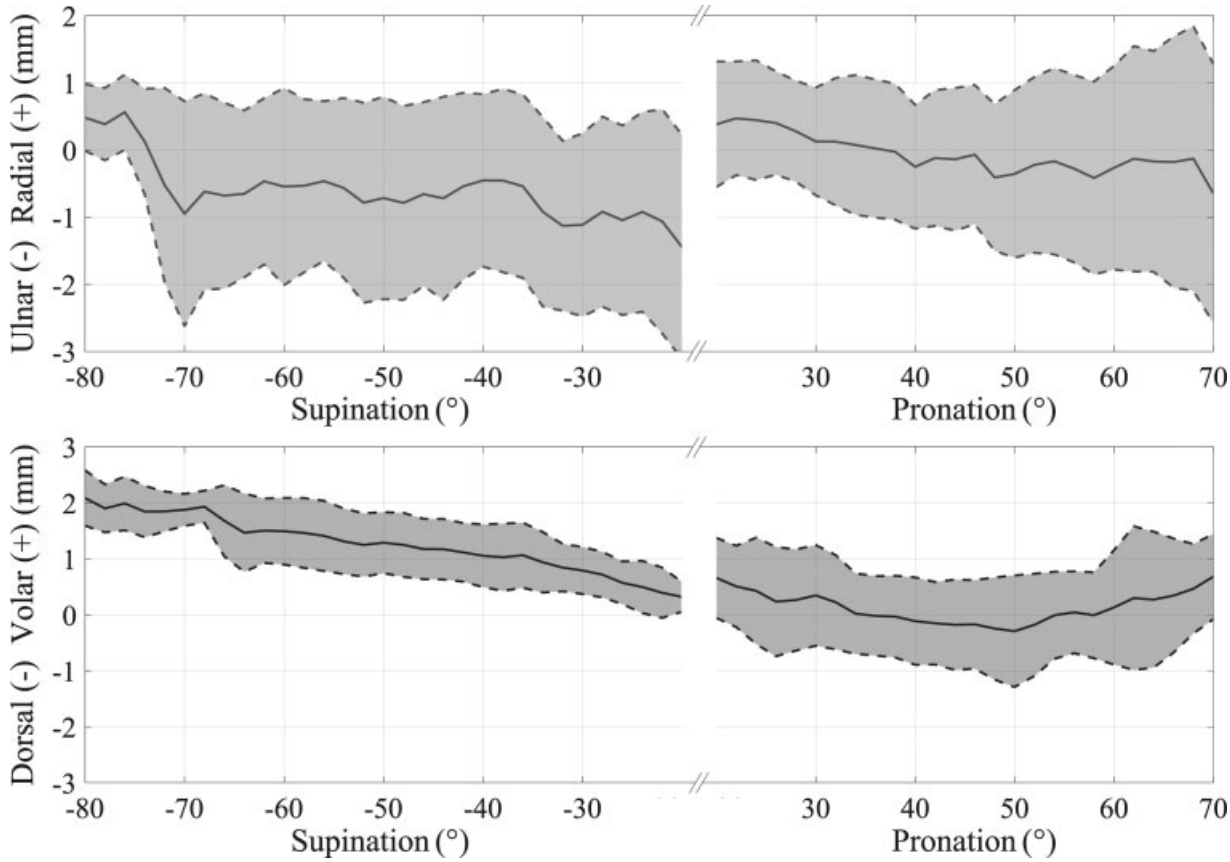

Fig. 5 Center of rotation (COR) moved volarly in supination, but it was stationary throughout pronation. The solid lines demonstrate the average COR location at every 2 degrees of pronation or supination, and the dashed lines demonstrate the standard deviation.

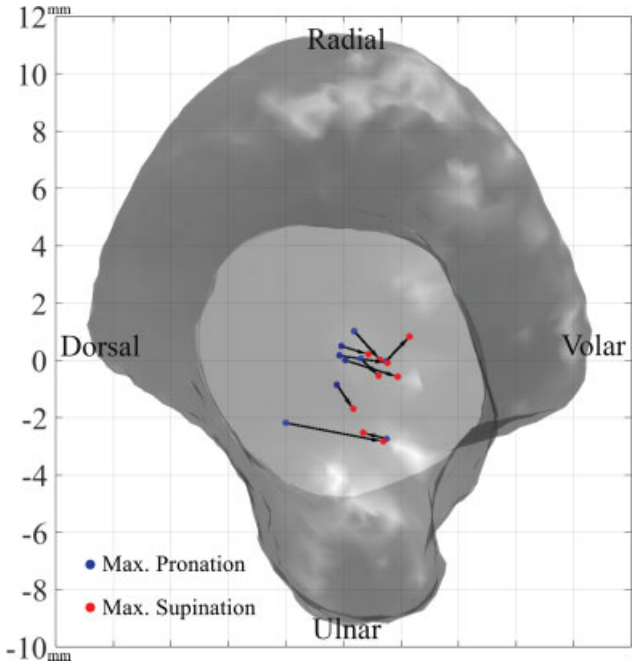

Fig. 6 Center of rotation moved volarly for eight (out of nine) participants from maximum pronation to maximum supination. Each arrow is directed from maximum pronation to maximum supination.

supination, and not continuously for each subject as we did in this study. Therefore, they were not able to detect a meaningful relationship between UV and pronosupination of individuals to understand the actual nonlinear relationship.[23] Lastly, Yeh et al studied radiographs of the forearms of 15 subjects and found a significant difference between the UV measured in pronation and neutral, but not neutral and supination, possibly due to the inaccuracies of UV measurement manually from the radiographs.[24] However, our submillimeter accuracy in measuring UV enabled us to demonstrate a 3.1 ± 1.6 mm change in UV from maximum pronation to maximum supination.

The COR location of DRUJ is not stationary, and as a previous study has described, it changes even with elbow flexion.[20] In this study we also demonstrated that the DRUJ COR changes during forearm rotation. The dynamic COR and the polynomial behavior of the UV at the DRUJ suggests that the DRUJ is moving during PS. Linked DRUJ replacement implants designed to stabilize an unstable or arthritic joint transform the DRUJ into a ball and socket articulation,[8] only allowing pure rotation and not the volar-dorsal translation that we found in this study. Although short-term outcomes have been promising,[8,45] altered kinematics of the DRUJ may lead to increased bone-implant stress and loosening or implant fracture in the long-term. Incorporating the COR and the UV translation into articulation design might help create a truly anatomical joint replacement.

There were some limitations to this study. Although the subjects were guided to hold their elbow in 90 degrees flexion, we were unable to control the exact degree of elbow flexion while the subjects performed the tasks of forearm rotation. Previous studies have mentioned the effect of elbow flexion on the UV and COR,[20] but these changes are only

significant when elbow moves from fully flexed position to fully extension. Thus, we believe our results are largely unaffected by this variation. Additionally, we were limited by the relatively small sample size and the homogenous nature of the subject's age and sex. Measured from the posteroanterior radiograph,[46] total configuration of the DRUJ of all of our participants was type II (oblique) and within range of 7.4 to 17.6 degrees. Although for the subjects included in the study a consistent pattern was noted for the UV and the COR changes, a larger sample size may provide an argument for a generalizable dataset. The shape of the sigmoid notch also varies in populations,[46] and large databases might be helpful in associating these variations to the COR changes.

In this study, we evaluated the motion of DRUJ by specifically observing UV and COR changes seen with forearm rotation. Our measurements of UV demonstrated a consistent, nonlinear behavior among all subjects, and a model was developed to standardize and calculate UV as a factor of the forearm rotation. COR did not change significantly in pronation, but it translated volarly during supinations.

Funding
J.J.C reports grants from National Institute of General Medical Sciences (P30GM122732), and from the American Foundation for Surgery of the Hand (AFSH) during the conduct of the study.

Conflict of Interest
None declared.

Acknowledgment
The authors thank Erika Tavares for her help throughout the biplanar videoradiography data acquisition.

References

1 Linscheid RL. Biomechanics of the distal radioulnar joint. Clin Orthop Relat Res 1992;(275):46–55
2 Shaaban H, Giakas G, Bolton M, Williams R, Scheker LR, Lees VC. The distal radioulnar joint as a load-bearing mechanism—a biomechanical study. J Hand Surg Am 2004;29(01):85–95
3 Epner RA, Bowers WH, Guilford WB. Ulnar variance—the effect of wrist positioning and roentgen filming technique. J Hand Surg Am 1982;7(03):298–305
4 Friedman SL, Palmer AK. The ulnar impaction syndrome. Hand Clin 1991;7(02):295–310
5 Laino DK, Petchprapa CN, Lee SK. Ulnar variance: correlation of plain radiographs, computed tomography, and magnetic resonance imaging with anatomic dissection. J Hand Surg Am 2012;37 (01):90–97
6 Palmer AK, Werner FW. The triangular fibrocartilage complex of the wrist—anatomy and function. J Hand Surg Am 1981;6(02):153–162
7 Sammer DM, Rizzo M. Ulnar impaction. Hand Clin 2010;26(04): 549–557
8 Palmer AK, Werner FW. Biomechanics of the distal radioulnar joint. Clin Orthop Relat Res 1984;(187):26–35
9 Calcagni M, Giesen T. Distal radioulnar joint arthroplasty with implants: a systematic review. EFORT Open Rev 2017;1(05):191–196
10 Herzberg G, Burnier M, Marc A, Izem Y. Primary wrist hemiarthroplasty for irreparable distal radius fracture in the independent elderly. J Wrist Surg 2015;4(03):156–163
11 Mikkelsen SS, Lindblad BE, Larsen ER, Sommer J. Sauvé-Kapandji operation for disorders of the distal radioulnar joint after Colles' fracture. Good results in 12 patients followed for 1.5-4 years. Acta Orthop Scand 1997;68(01):64–66
12 Degreef I, De Smet L. The Scheker distal radioulnar joint arthroplasty to unravel a virtually unsolvable problem. Acta Orthop Belg 2013;79(02):141–145
13 Strigel RM, Richardson ML. Distal radioulnar joint arthroplasty with a Scheker prosthesis. Radiol Case Rep 2015;1(02):66–68
14 Tulipan DJ, Eaton RG, Eberhart RE. The Darrach procedure defended: technique redefined and long-term follow-up. J Hand Surg Am 1991;16(03):438–444
15 Banks SA, Hodge WA. Implant design affects knee arthroplasty kinematics during stair-stepping. Clin Orthop Relat Res 2004; (426):187–193
16 Gregory TM, Sankey A, Augereau B, et al. Accuracy of glenoid component placement in total shoulder arthroplasty and its effect on clinical and radiological outcome in a retrospective, longitudinal, monocentric open study. PLoS One 2013;8(10):e75791
17 Galbusera F, Anasetti F, Bellini CM, Costa F, Fornari M. The influence of the axial, antero-posterior and lateral positions of the center of rotation of a ball-and-socket disc prosthesis on the cervical spine biomechanics. Clin Biomech (Bristol, Avon) 2010; 25(05):397–401
18 Lecerf G, Fessy MH, Philippot R, et al. Femoral offset: anatomical concept, definition, assessment, implications for preoperative templating and hip arthroplasty. Orthop Traumatol Surg Res 2009;95(03):210–219
19 Matsuki KO, Matsuki K, Mu S, et al. In vivo 3D kinematics of normal forearms: analysis of dynamic forearm rotation. Clin Biomech (Bristol, Avon) 2010;25(10):979–983
20 Tay SC, van Riet R, Kazunari T, Amrami KK, An K-N, Berger RA. In-vivo kinematic analysis of forearm rotation using helical axis analysis. Clin Biomech (Bristol, Avon) 2010;25(07):655–659
21 Fu E, Li G, Souer JS, et al. Elbow position affects distal radioulnar joint kinematics. J Hand Surg Am 2009;34(07):1261–1268
22 Bellevue KD, Thayer MK, Pouliot M, Huang JI, Hanel D. Complications of aptis DRUJ arthroplasty. J Hand Surg Am 2017;42(09):S14–S15
23 Jung JM, Baek GH, Kim JH, Lee YH, Chung MS. Changes in ulnar variance in relation to forearm rotation and grip. J Bone Joint Surg Br 2001;83(07):1029–1033
24 Yeh GL, Beredjiklian PK, Katz MA, Steinberg DR, Bozentka DJ. Effects of forearm rotation on the clinical evaluation of ulnar variance. J Hand Surg Am 2001;26(06):1042–1046
25 Baeyens J-P, Van Glabbeek F, Goossens M, Gielen J, Van Roy P, Clarys J-P. In vivo 3D arthrokinematics of the proximal and distal radioulnar joints during active pronation and supination. Clin Biomech (Bristol, Avon) 2006;21(Suppl 1):S9–S12
26 Abe S, Otake Y, Tennma Y, et al. Analysis of forearm rotational motion using biplane fluoroscopic intensity-based 2D-3D matching. J Biomech 2019;89:128–133
27 Akhbari B, Morton A, Moore D, Weiss AC, Wolfe SW, Crisco J. Kinematic accuracy in tracking total wrist arthroplasty with biplane videoradiography using a CT-generated model. J Biomech Eng 2019;141(04):0445031–0445037
28 Akhbari B, Morton AM, Moore DC, Weiss AC, Wolfe SW, Crisco JJ. Accuracy of biplane videoradiography for quantifying dynamic wrist kinematics. J Biomech 2019;92:120–125
29 Anderst W, Zauel R, Bishop J, Demps E, Tashman S. Validation of three-dimensional model-based tibio-femoral tracking during running. Med Eng Phys 2009;31(01):10–16
30 Bey MJ, Kline SK, Tashman S, Zauel R. Accuracy of biplane X-ray imaging combined with model-based tracking for measuring in-vivo patellofemoral joint motion. J Orthop Surg Res 2008;3:38
31 Bey MJ, Zauel R, Brock SK, Tashman S. Validation of a new model-based tracking technique for measuring three-dimensional, in vivo glenohumeral joint kinematics. J Biomech Eng 2006;128(04): 604–609

32 Miranda DL, Schwartz JB, Loomis AC, Brainerd EL, Fleming BC, Crisco JJ. Static and dynamic error of a biplanar videoradiography system using marker-based and markerless tracking techniques. J Biomech Eng 2011;133(12):121002
33 Tashman S, Anderst W. In-vivo measurement of dynamic joint motion using high speed biplane radiography and CT: application to canine ACL deficiency. J Biomech Eng 2003;125(02):238–245
34 Akhbari B, Morton AM, Shah KN, et al. Proximal-distal shift of the center of rotation in a total wrist arthroplasty is more than twice of the healthy wrist. J Orthop Res 2020;38(07):1575–1586
35 Moore DC, Hogan KA, Crisco JJ III, Akelman E, Dasilva MF, Weiss A-PC. Three-dimensional in vivo kinematics of the distal radioulnar joint in malunited distal radius fractures. J Hand Surg Am 2002;27 (02):233–242
36 Knörlein BJ, Baier DB, Gatesy SM, Laurence-Chasen JD, Brainerd EL. Validation of XMALab software for marker-based XROMM. J Exp Biol 2016;219(Pt 23):3701–3711
37 Miranda DL, Rainbow MJ, Crisco JJ, Fleming BC. Kinematic differences between optical motion capture and biplanar videoradiography during a jump-cut maneuver. J Biomech 2013;46(03):567–573
38 Broga D. Ionizing radiation exposure of the population of the United States. Med Phys 2009;36(11):5375–5375
39 Akhbari B, Moore DC, Laidlaw DH, et al. Predicting carpal bone kinematics using an expanded digital database of wrist carpal bone anatomy and kinematics. J Orthop Res 2019;37(12): 2661–2670
40 Crisco JJ, Coburn JC, Moore DC, Akelman E, Weiss A-PC, Wolfe SW. In vivo radiocarpal kinematics and the dart thrower's motion. J Bone Joint Surg Am 2005;87(12):2729–2740
41 Kennedy J, Eberhart R. Particle swarm optimization. Paper presented at: Proceedings of the IEEE International Conference on Neural Networks Piscataway, NJ: IEEE Press; 1995:1942–1948
42 Panjabi M, White AA III. A mathematical approach for three-dimensional analysis of the mechanics of the spine. J Biomech 1971;4(03):203–211
43 Tay SC, Berger RA, Tomita K, Tan ET, Amrami KK, An K-N. In vivo three-dimensional displacement of the distal radioulnar joint during resisted forearm rotation. J Hand Surg Am 2007;32(04): 450–458
44 Gilula LA, Mann FA, Dobyns JH, Yin Y. Wrist terminology as defined by the International Wrist Investigators' Workshop (IWIW). J Bone Joint Surg 2002;84:1–66
45 Kachooei AR, Chase SM, Jupiter JB. Outcome assessment after aptis distal radioulnar joint (DRUJ) implant arthroplasty. Arch Bone Jt Surg 2014;2(03):180–184
46 Tolat AR, Stanley JK, Trail IA. A cadaveric study of the anatomy and stability of the distal radioulnar joint in the coronal and transverse planes. J Hand Surg [Br] 1996;21(05):587–594